

BUSBAR SIZING MODELING TOOLS: COMPARING AN ANSYS® BASED 3D MODEL WITH THE VERSATILE 1D MODEL PART OF MHD-VALDIS

Marc Dupuis¹ and Valdis Bojarevics²

¹GéniSim Inc.
3111 Alger St., Jonquière, Québec, Canada, G7S 2M9
marc.dupuis@genisim.com

²University of Greenwich, School of Computing and Mathematics
30 Park Row, London, SE10 9LS, UK
V.Bojarevics@gre.ac.uk

Keywords: Thermo-electric models, MHD models, Aluminum electrolysis cell

Abstract

The main goal of a cell stability MHD model like MHD-Valdis is to help locate the busbars around the cell in a way that leads to the generation of a magnetic field inside the cell that itself leads to a stable cell operation.

Yet, as far as the cell stability is concerned, the uniformity of the current density in the metal pad is also extremely important and can only be achieved with a correct busbar network sizing.

This work compares the usage of a detailed ANSYS® based 3D thermo-electric model with the one of the versatile 1D model part of MHD-Valdis to help design a well balanced busbar network.

Introduction

The problem of choosing the busbar sizing in order to obtain a uniform current pick up in all the collector bars of a modern side by side high amperage aluminum electrolysis cell, while known to be critical to the cell MHD stability, is not often discussed in the literature.

References [1 and 2] are two exceptions, each presents an in-house computer code called respectively NEWBUS and BUSCAL designed specifically to do such a task. Both use a simple 1D line busbar network representation, a temperature dependent electrical resistivity and solve for the resulting non-linear problem by computing the voltage and temperature equations iteratively and alternately until convergence is reached. These days, such an in-house solver can be setup fairly rapidly in an Excel spreadsheet (see figure 1).

Typically, the calculated collector bars current pick up distribution and the different currents in the busbar network are then transferred to the metal pad current density solver and the metal pad magnetic field solver in preparation to run the MHD wave stability solver.

Much more recently, [3, 4, 5 and 6] ANSYS® based 3D full cell and external busbar thermo-electric models have been developed in order to very accurately compute the metal pad current density field considering both the converged steady-state ledge profile and the busbar design. Of course, once developed, the 3D busbar model can also be solved stand-alone.

a*(1+b*T)	a	b	ql (w) =	294.79				
				118.93	0.064			
ka (w/mC) =	215	0	tm =	143.3397	h (m) =	1.1		
ks (w/mC) =	48	0	ra =	4.79E-08	t (m) =	0.15		
ra (ohm-m) =	3.00E-08	0.0038	r (ohm-m) =	2.87E-06	w (m) =	0.12		
rs (ohm-m) =	1.10E-07	0.01	amp =	7900	p (m) =	0.54		
ha (w/m2C) =	6	0.0064	jh (w) =	161.65	s (m2) =	0.018		
Tair(C) =	25		qc (w) =	213.97				
			tm =	219.3407	tm =	219.3407	l (m) =	0.45
l (m) =	0.45		rs =	3.51E-07	rs =	3.51E-07	rs =	0.45
h (m) =	0.16		r (ohm) =	9.88E-06	r (ohm) =	9.88E-06	h (m) =	0.16
w (m) =	0.1		amp =	2294	amp =	2294	w (m) =	0.1
p (m) =	0.52		jh (w) =	51.99	jh (w) =	51.99	p (m) =	0.52
s (m2) =	0.016		qc (w) =	135.14	qc (w) =	135.14	s (m2) =	0.016
			ql (w) =	1252.14	ql (w) =	1252.14		
				179.749	0.043	258.93	0.020	
tm =	404.4655		tm =	349.8743	tm =	404.4655		
rs =	5.55E-07		rs =	4.95E-07	rs =	5.55E-07		
r (ohm) =	8.80E-06		r (ohm) =	7.85E-06	r (ohm) =	8.80E-06		
amp =	2294		amp =	2912	amp =	2294		
jh (w) =	46.32		jh (w) =	66.55	jh (w) =	46.32		
qc (w) =	860.89		qc (w) =	1029.74	qc (w) =	860.89		
	550	0		520	0.02	550	0	
h (m) =	0.36		h (m) =	0.36	h (m) =	0.36		
d (m) =	0.17		d (m) =	0.17	d (m) =	0.17		
p (m) =	0.534071		p (m) =	0.534071	p (m) =	0.534071		
s (m2) =	0.022698		s (m2) =	0.022698	s (m2) =	0.022698		

Figure 1. Simple 1D line network model of an anode studs, yoke and rod implemented in an Excel spreadsheet.

So, on one hand, it is possible to develop an in-house code to solve a simplified 1D line network busbar representation and use that tool to perform busbar sizing optimization and, on the other hand, it is possible to develop an ANSYS® based parametric 3D busbar model to do the same.

Yet, there is now also a third option, using MHD-Valdis [7, 8, 9, 4, 5 and 10] which is a commercially available, fully non-linear MHD cell stability solver. The fact that it is fully non-linear, means that it is solving among other variables the busbar network current distribution at each time step. It is doing so using a versatile 1D line network busbar generator and solver called BUSNET also available to carry out busbar sizing optimization studies.

The three above options will be compared to try to identify the most efficient tool to carry out busbar sizing optimization studies, but before proceeding with the comparison exercise, it is important to take a step back and first review the background theory of the equations that need to be solved.

Busbar Heat Balance and Voltage Drop Equations

In steady-state mode, the busbar network heat balance equations are:

$$A(m^2) = 2 \times (H + W) \times L \quad (1)$$

$$S(m^2) = H \times W \quad (2)$$

$$R(\text{ohm}) = \frac{\rho(T_B) \times L}{S} \quad (3)$$

$$\rho(\text{ohm} \cdot m) = \rho_0 \times (1 + \alpha_\rho \times T_B) \quad (4)$$

$$R \times I^2 (W) = \frac{k}{L} \times S \times (T_B - T_N) + h(T_B) \times A \times (T_B - T_{air}) \quad (5)$$

Both references [1 and 2] correctly introduced all the above equations including equation (4): the temperature dependent electrical resistivity of the aluminium busbar that makes that system of equations non-linear.

But both references [1 and 2] failed to present an equation for h , the global (convective and radiative) heat transfer coefficient between the busbar external surfaces and its surrounding environment.

That global heat transfer coefficient can be evaluated as below assuming that the background radiative temperature is equal to T_{air} the nearby air temperature [11, 12]:

$$h(W / m^2 \cdot ^\circ C) = h_C(T_B) + h_R(T_B) \quad (6)$$

$$h_C(W / m^2 \cdot ^\circ C) = \frac{Nu \times k_{film}}{L} \quad (7)$$

$$h_R(W / m^2 \cdot ^\circ C) = \epsilon \sigma (T_B + T_{air})(T_B^2 + T_{air}^2) \quad (8)$$

Notice that in eq. (8) both T_B and T_{air} are in K.

In equation (7) Nu , the Nusselt number is correlated with Ra , the Rayleigh number using the following semi-empirical relationships.

For vertical surfaces, we have:

$$Nu = 0.59 Ra^{1/4}, \text{ for } 10^4 \leq Ra \leq 10^9 \quad (9)$$

$$Nu = 0.105 Ra^{1/3}, \text{ for } 10^9 \leq Ra \leq 10^{12} \quad (10)$$

For horizontal surfaces facing up we have:

$$Nu = 0.54 Ra^{1/4}, \text{ for } 10^5 \leq Ra \leq 2 \times 10^7 \quad (11)$$

$$Nu = 0.141 Ra^{1/3}, \text{ for } 10^7 \leq Ra \leq 10^{11} \quad (12)$$

And finally, for horizontal surfaces facing down we have:

$$Nu = 0.27 Ra^{1/4}, \text{ for } 3 \times 10^5 \leq Ra \leq 3 \times 10^{10} \quad (13)$$

Where:

$$Ra = \frac{g \beta L^3 (T_B - T_{air})}{\nu^2} \times Pr \quad (14)$$

Once tabulated for one value of T_{air} and the range of possible values for T_B , it is possible to fit the results obtained computing the above complex set of equations into the following form (see figure 2):

$$h(W / m^2 \cdot ^\circ C) = h_0 \times (1 + \alpha_h \times T_B) \quad (15)$$

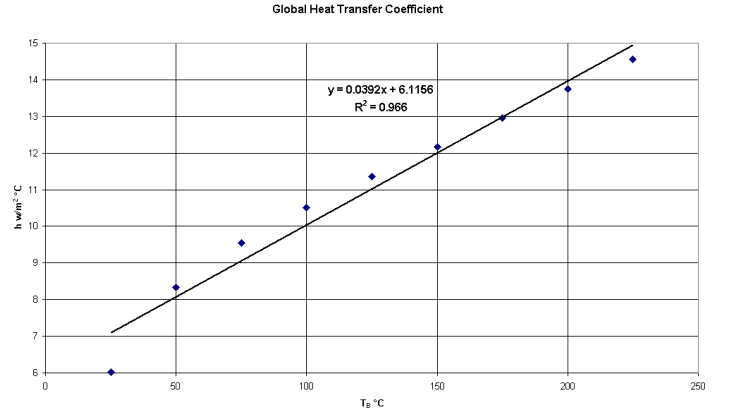


Figure 2. Curve fitting of h for one value of T_{air} and \mathcal{E} .

It is very important to realize that the correct evaluation of equation (15) is critical to the correct calculation of the different busbar temperatures in the network and that equation (15) coupled with equation (4) will dictate what will be the final busbar network current balance.

In order to even better illustrate the importance of equation (15), it is possible in the case of a very long busbar of constant cross section to neglect the heat conduction term in the middle part of that busbar. The temperature in the middle section of that busbar is simply define by the following equation:

$$\frac{\rho_0 \times (1 + \alpha_\rho \times T_B)}{S} \times I^2 = h_0 \times (1 + \alpha_h \times T_B) \times P \times (T_B - T_{air}) \quad (16)$$

Where:

$$P(m) = 2 \times (H + W) \quad (17)$$

Or more directly, it is possible to rewrite (16) as:

$$T_B = \frac{\rho_0 \times (1 + \alpha_\rho \times T_B) \times I^2}{h_0 \times (1 + \alpha_h \times T_B) \times P \times S} + T_{air} \quad (18)$$

By assigning some values to the 8 parameters involved:

$$\rho_0 = 1E-8; \quad \alpha_\rho = 0.0038;$$

$$h_0 = 6; \quad \alpha_h = 0.0064;$$

$$S = 0.1; \quad P = 1.4;$$

$$I = 50000; \quad T_{air} = 25$$

T_B converges to 100 °C. But if by applying a surface treatment to that busbar surface, the surface emissivity is increased from 0.4 to 1.0, the heat transfer coefficient equation parameters are changing to:

$$h_0 = 8.6; \quad \alpha_h = 0.0077$$

And T_B now converges to 76 °C reducing the busbar electrical resistivity by 7%!

The voltage equation is a lot more straightforward as it is the standard application of the Kirchoff's laws:

$$R \times I \text{ (V)} = (V_B - V_N) \quad (19)$$

$$\sum I = 0 \text{ at any given node in the network} \quad (20)$$

It is a linear problem when the temperatures are kept constant.

3D ANSYS® based busbar model

It is quite easy to build a parametric 3D ANSYS® based busbar model (see figure 3). In such a model, the exact busbar geometry can be reproduced and the detailed convection and radiation boundary conditions can be applied i.e. different boundary conditions for the vertical, horizontal facing up and down surfaces etc.

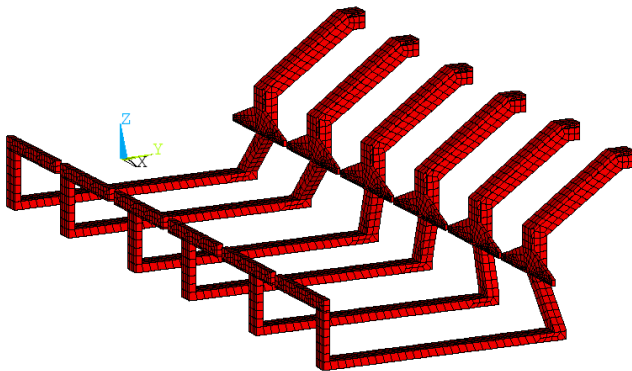


Figure 3. Mesh of the 3D ANSYS® based busbar model.

In the 3D model presented here however, in order to be able to compare with the 1D model results, equation (15) have been used to compute all the heat transfer coefficients instead of using the standard COEF macro [11] that computes a series of heat transfer coefficients tables using the above full set of equations based on individual surface orientation, typical length etc. So here, for comparison purpose only, a single heat transfer coefficient equation is wrongly used for all the busbar external surfaces regardless of the different surface orientations.

All the busbar surfaces in contact with cathodic flexibles are defined to be at 0 potential and the surfaces of the 12 risers in contact with the anode beam have been coupled together in order to be at the same potential. Figure 4 presents the obtained temperature and figure 5 presents the obtained voltage.

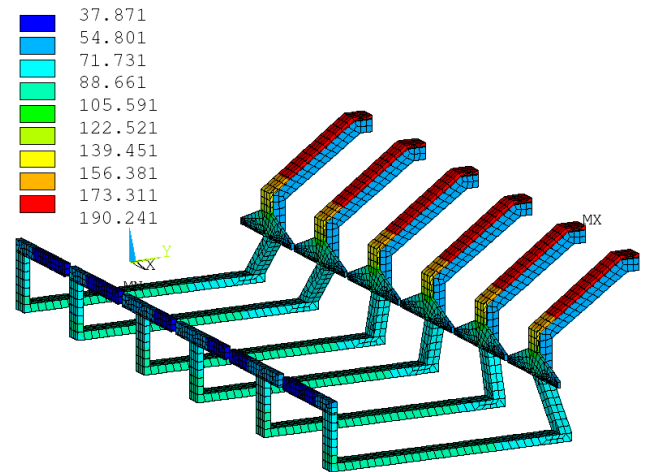


Figure 4. Thermal solution of the 3D ANSYS® based busbar model.

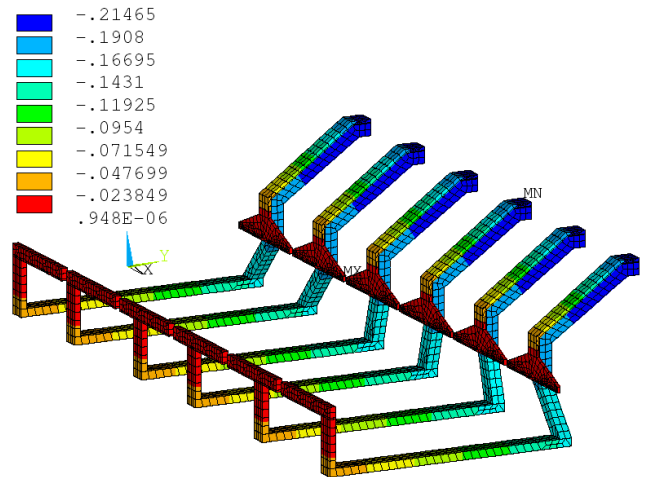


Figure 5. Voltage solution of the 3D ANSYS® based busbar model.

The maximum temperature reached in the positive or upstream busbar is 95.1 °C and in the negative or downstream busbar is 190.2 °C. The global busbar network voltage drop is 215 mV with 243.3 kA or 48.7% of the total 500 kA passing in the negative or downstream side and 256.7 kA or 51.3% passing in the positive or upstream side.

1D ANSYS® based busbar model

Like NEWBUS [1] and BUSCAL [2], it is possible to write a FORTRAN program to solve the coupled voltage and temperature set of non-linear equations generated from the discretisation of a 3D busbar network geometry into a network of 1D line elements. Nowadays, it is also possible to create an Excel spreadsheet similar to the one presented in figure 1.

But building a versatile and user friendly in-house application takes time. For efficiency reasons, it was decided to use 1D thermo-electric line elements available in ANSYS® to build a 1D line elements network model similar to NEWBUS and BUSCAL (see figure 6).

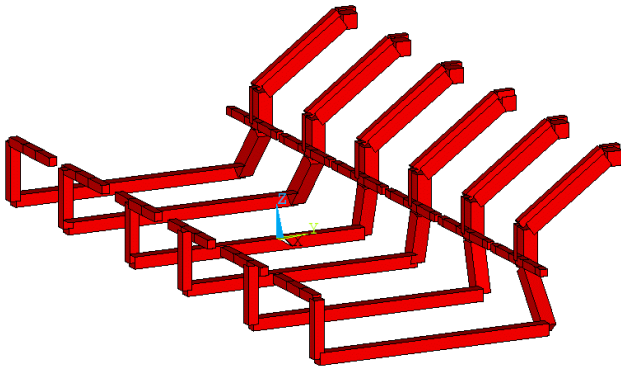


Figure 6. Mesh of the 1D ANSYS® based busbar model.

The model contains 108 line elements and 120 nodes. Except for the V shaped current collectors at the base of the negative risers, each busbar has been represented by a 1D line element of identical section and length. The external busbar surface area needs to be calculated as an element property and again except for the V shaped negative current collectors those surface areas are also identical to the one automatically computed by ANSYS® in the 3D busbar model. Of course, the aluminum busbar material properties and the boundary conditions are identical to the one set in the 3D model.

The maximum temperature reached in the positive busbar is 98.4 °C and in the negative busbar is 186.0 °C. The global busbar network voltage drop is 230 mV with 235.6 kA or 47.1% passing in the negative side and 264.4 kA or 52.9% passing in the positive side.

By comparing the results between the 3D and the 1D model, it appears obvious that the negative risers section is more resistive in the 1D model version. Clearly the 1D line elements representation of the V shaped current collectors, which is really a 2D feature, is not accurately enough represented.

It is of course possible to improve the 1D model representation of the V shaped negative current conductors (now that it is known that it is required to do so following the comparison exercise). This only requires the construction of a more complex 1D line elements network (see figure 7).

In this improved 1D model version, the maximum temperature reach in the positive busbar is 95.5 °C and in the negative busbar is 190.9 °C. The global busbar network voltage drop is 224 mV with 241.2 kA or 48.2% passing in the negative side and 258.8 kA or 51.8% passing in the positive side.

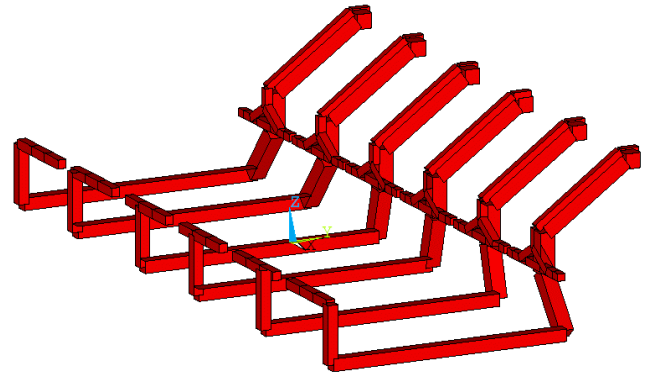


Figure 7. Improved mesh of the 1D ANSYS® based busbar model.

This is clearly a better representation of the real 3D busbar network but still some discrepancies remain. This comparison exercise highlights very well that it is not that easy to perfectly represent a real 3D busbar geometry using only a 1D line elements discretisation. But considering that little loss of accuracy, is the 1D ANSYS® based model a more efficient tool to carry out busbar sizing optimization studies compared to the 3D ANSYS® based model?

It takes of course a lot more efforts to build a 3D model geometry than a 1D model geometry. An even if it is possible to build a parametric 3D model, there is a limit in the versatility of a single model topology i.e. it will not be possible to analyze all the possible busbar configuration one might want to analyze using a single 3D model topology. So using the 3D ANSYS® based model will translate into long delays spent in building different 3D busbar configuration model topology often to use them only a few times! This is clearly not a very practical approach.

Unfortunately, using an ANSYS® based 1D line elements model is not a very practical solution either because ANSYS® is not offering a convenient way to apply the global heat transfer boundary conditions. Each busbar external surface area must be calculated manually by the model developer and input as a material property.

This means that without creating a macro to streamline the model setup task, it would be very cumbersome to use that approach to carry out a busbar sizing optimization study. So neither the 3D ANSYS® based model and the 1D ANSYS® based model would be the efficient and versatile tool required.

Versatile 1D busbar model part of MHD-Valdis

MHD-Valdis is a fully non-linear MHD cell stability solver that was initially developed as an in-house code for the former USSR aluminum industry and later adapted for the in-house use at Reynolds Metals. But it has now become available, quite exceptionally, as a commercial software of certain unique advantages. Because it is a specialized MHD cell stability solver, it has been designed to perform this single task efficiently. Being a commercial package, it is quite user friendly and comes with customer training and support if required.

The data input for the network current modeling and the magneto-hydrodynamic programs are unified. The MHD package generates the very large set of Kirchhoff equations set automatically from the relatively simple unified data input. The computed temperatures of the electrically heated bars permit to accommodate to the resistivity changes. Additional flexibility permits to simulate anode changes,

disconnected cathode bars, various branching of the current path between the cells, etc.

The development of the program is based on the previous experience in the current simulation programs: NEWBUS [1], reports from Reynolds Metals Company, and Russian program TOK from the VAMI institute. Current distribution in a busbar network can be described to a reasonable approximation accuracy suitable for engineering purposes by linear resistance elements. The electric currents and voltages in such a circuit are governed by the Kirchhoff laws:

1) the **voltage law**: The algebraic sum of the potential differences taken around a loop (or 'mesh') of a circuit is zero;

2) the **current law**: The algebraic sum of the currents into a node of a circuit is zero.

Directly applied, these laws contain unknown potential differences for each resistance and unknown currents for each mesh of a given circuit. There are two methods to reduce the number of independent unknowns and the equations respectively. These are based on combining the two laws and are referred to as either mesh analysis or nodal analysis. The mesh analysis is based on currents as unknowns. A set of mesh currents I_n are chosen to traverse all complete loops of the circuit. Since each mesh current flows right through any junction (node) in its path, the current law is automatically satisfied. Then it is left to apply the voltage law for each of the meshes by replacing the potential differences with the algebraic sums of currents through the particular resistance multiplied by this resistance (Ohms law).

For the reduction cell situation this procedure was used in the previously referenced programs and involves a tedious job of locating all possible meshes of the circuit that is rather hard to automate in a computer program. Therefore this approach involves an intelligent input from the program user and results in long labor days with a possibility of potential errors. Principal changes in the circuit, such as anode or cathode element disconnection or new branching, require significant reconsideration of the equation set.

For the automatic circuit analysis purposes the nodal analysis is found to be more convenient. According to this method the potentials at the nodes are the independent unknowns. The use of node potentials rather than mesh currents makes for greater efficiency in the analysis of circuits that are predominantly parallel in character, since the number of simultaneous equations that have to be solved is significantly smaller. The following equation set arises for M nodes each of which has N directly connected neighbor resistances:

$$U_m \sum_{n=1}^N \frac{1}{R_n} - \sum_{n=1}^N \frac{U_n}{R_n} = I_m \quad , \quad (21)$$

where U_m is potential at a node, U_n - for nodes at other ends of neighbor bars, R_n - resistances of neighbor bars, I_m - external current entering the node. In our case total current 'I' enters the reference nodes in the liquid metal of previous cell and '-I' current leaves the nodes at the liquid metal of the downstream cell. For all other nodes the external current - right side of the equation - is zero. This is just another statement of the current law, and the voltage law is satisfied because the sum of the potential differences, with U_m expressed from (21), over the closed mesh is identically zero. Formally this law can be applied even for two resistances connected in series, and this property is essential in order to generate automatically the set of equations to solve.

After finding the potentials at nodes, the potential difference between two neighbor nodes multiplied by the connecting resistance gives the current in each resistance. The main task of the present program is to find the current distribution in the bar network, yet a further improvement in accuracy can be achieved if computing Joule heating: $R_m \cdot I_m^2$ for each of the resistance elements.

Knowing the Joule heating, it is possible to estimate the temperature of a bar. For this purpose we integrate the temperature T equation over a single bar volume and an equation set for the discrete variables yields:

$$\sum_n \frac{k_m \cdot (T_m - T_n) \cdot S_m}{L_m} + h_m \cdot A_m \cdot (T_m - T_{air}) = R_m I_m^2 \quad (22)$$

Where k_m is conductivity of the m-th bar, summation is over n neighbor bars, S_m is the cross section area, L_m - length, h_m from (15). When the temperatures are calculated, the resistances $R_m(T)$ can be updated taking into account the linear temperature dependence (4). This set can also be solved by linear algebra solvers, e.g., from the package LAPACK.

After this new resistances are calculated and the electric circuit equation set solved again to iterate the whole procedure while the convergence is achieved. The convergence is easily established for bars with reasonable cross sections and sufficiently effective heat transfer to the ambient air and to the neighbor bars. We incorporate in the program also the heating at the ends of first and last bars connected to the anodes and the cathode carbon by assigning the user defined temperatures at these ends.

The first calculation step needed for an MHD model is the electric current distribution in the busbars. This is calculated by coupling the electric current in the fluid zone to the resistance network representing the elements division of individual anodes and cathode collector bars as well as the whole busbar circuit between two adjacent cells. The electric current in the fluid zones must be computed from the continuous media equations governing the DC current (which can change in time with the waves and anode burnout process):

$$\mathbf{j} = -\sigma \nabla \phi + \sigma \mathbf{v} \times \mathbf{B}, \quad (23)$$

where the induced currents in the highly conducting liquid metal are accounted for. The electric potential in the fluid is governed by the equation:

$$\nabla^2 \phi = \nabla \cdot (\mathbf{v} \times \mathbf{B}), \quad (24)$$

and the boundary conditions of zero current at the insulating walls, given current distribution j_a at anodes, j_c at cathode carbon (both supplied from the linear element resistivity network solution, which in turn is coupled to the computed potential distribution from (24)). At the interface between the liquid metal and the electrolyte the continuity of the potential and the electric current normal component must be satisfied.

As the first step toward the solution of the cell MHD stability, MHD-Valdis uses the versatile 1D line element busbar network generator called BUSNET to create the 1D busbar mesh reading a very compact user input file. Then in a few seconds, it solves the non-linear problem and generates a TECPLOT [13] compatible output file and a standard printout ASCII output file called BARSOUT.

For the present example, the MHD-Valdis BUSNET user input file reproduces exactly the same busbar geometry as the second 1D

ANSYS® model. Yet, it is important to realize that BUSNET is creating and solving a lot more than the busbar network, it is creating and solving the full cell network as well (see figure 8). BUSNET results are as follow: the maximum temperature reached in the positive busbar is 94°C and in the negative busbar is 197 °C; the global busbar network drop is 224 mV with 247.0 kA or 49.4% passing in the negative or downstream side and 253.0 kA or 50.6% passing in the positive or upstream side.

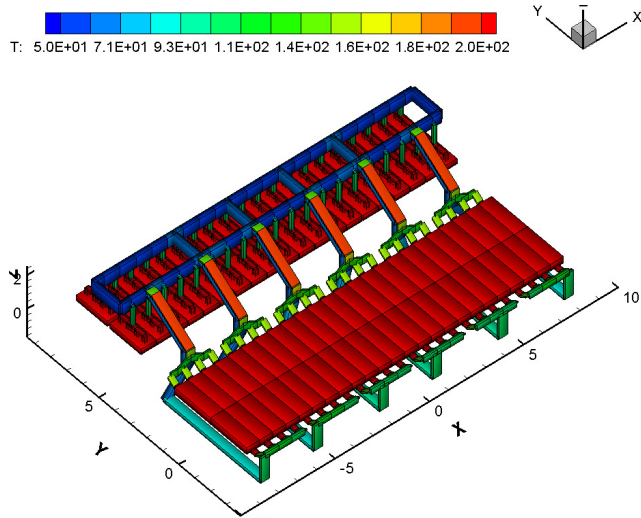


Figure 8. Thermal solution of the BUSNET full cell and busbar model.

The fact that the network current balance between the positive and negative sides is closer to 50% 50% than both the 3D and 1D ANSYS® models can easily be explained by the fact that by modeling also the cathode blocks, BUSNET is solving the problem more accurately because the true equipotential condition is at the metal pad above the cathode block. If the current distribution is not uniform between the positive and negative sides of the cell, the potential in the cathode flexibles will not be the same between the positive and negative sides and this of course have an impact on the current distribution itself.

This little comparison exercise just highlighted the fact that to accurately compute the busbar network current distribution, it is important to consider also the cathode block resistance layer as the two valid equipotential points are the metal pad and the anode beam not the cathode flexibles and the anode beam.

So from that fact alone, BUSNET the 1D versatile busbar model part of MHD-Valdis is a better tool to carry out a busbar sizing optimization study. But this is not the only reason, BUSNET user input file is also quite easy to edit and TECPLOT is a powerful and easy to learn postprocessor, making BUSNET a user friendly tool to use.

Conclusions

It was demonstrated that it is not possible to reduce a given 3D busbar geometry into a 1D line elements network geometry without losing some accuracy.

It was demonstrated that the global heat transfer coefficient between the busbar external surfaces and its surrounding has a big impact on the busbar thermal balance. An improper setup of that temperature dependent parameter will affect significantly the accuracy of the model.

It was demonstrated that it is not possible to accurately compute the busbar network current balance without including the cathode blocks because the potential at the end of the cathode flexibles is itself influenced by the current balance.

Finally, MHD-Valdis is the modeling tool recommended to carry out a busbar sizing optimization study because it is very efficient, versatile and user friendly. The maximum accuracy will be obtained by using an ANSYS® based 3D full cell and external busbar model, but that tool is not at all practical to carry out an optimization study.

References

1. T. Tvedt and H. G. Nebell, "NEWBUS, a Simulation Program for Calculation of the Current Distribution in the Bus Bar System of Alumina Reduction Cells", *Light Metals, TMS*, (1988), 567-573.
2. J. I. Buiza, "Electromagnetic Optimization of the V-350 Cell", *Light Metals, TMS*, (1989), 211-214.
3. M. Dupuis, "Toward the Development of a 3D Full Cell and External Busbars Thermo-Electric Model", *Proceedings of the 41st Conference on Light Metal, CIM*, (2002), 25-39.
4. M. Dupuis, V. Bojarevics and J. Freibergs, "Demonstration Thermo-Electric and MHD Mathematical Models of a 500 kA Al Electrolysis cell: Part 2", *Light Metals, TMS*, (2004), 453-459.
5. M. Dupuis and V. Bojarevics, "Weakly Coupled Thermo-Electric and MHD Mathematical Models of an Aluminium Electrolysis Cell", *Light Metals, TMS*, (2005), 449-454.
6. M. Dupuis, "Thermo-Electric Design of a 740 kA Cell, is there a Size Limit?" *Aluminium 81*, (2005) 4, 324-327.
7. V. Bojarevics and M.V. Romerio, "Long Wave Instability of Liquid Metal-electrolyte Interface in Aluminium Electrolysis Cells: a Generalization of Sele's Criterion", *Eur. J. Mech., B/Fluids*, 13 (1) (1994), 33-56.
8. V. Bojarevics, "Non-Linear Waves with Electromagnetic Interaction in Aluminium Electrolysis Cells", *Progr. Fluid Flow Res.: Turbulence and Applied MHD*, eds. H. Branover and Y. Unger, AIAA, (1998), Chapter 58, 833-848.
9. M. Dupuis, V. Bojarevics and J. Freibergs, "Demonstration Thermo-Electric and MHD Mathematical Models of a 500 kA Al Electrolysis cell", *Proceedings of the 42nd Conference on Light Metals, CIM*, (2003), 3-20.
10. V. Bojarevics, "MHD-Valdis Reference Manual", *Greenwich University*, (2005).
11. M. Dupuis, "Computation of Heat Transfer Coefficient Tables Establishing Boundary Conditions between Hot Surfaces and their Surroundings", *GeniSim Internal report*, (1996).
12. M. Dupuis, A. Koshie, V. Janakiraman, S. Karthikeyan and D. Saravanan, "Accurate Assessment of the Hirakud Smelter Aluminium Reduction Cell Thermal Balance using only Temperature Measurements", *Proceedings of the 43rd Conference on Light Metals, CIM*, (2004), 525-533.
13. "TECPLOT User's Manual", *Amtec Engineering*, (2005), www.tecplot.com/support/tecplot_documentation.htm